THE JOURNAL OF PHYSICAL CHEMISTRY B

Article

pubs.acs.org/JPCB

Solvent Polarity Considerations Are Unable to Describe Fullerene Solvation Behavior

Vitaly V. Chaban,[†] Cleiton Maciel,[‡] and Eudes Eterno Fileti*[,§]

[†]MEMPHYS - Center for Biomembrane Physics, Odense M, 5230, Kingdom of Denmark

[‡]Centro de Ciências Naturais e Humanas, Universidade Federal do ABC, 09210-270 Santo André, São Paulo, Brazil

[§]Instituto de Ciência e Tecnologia, Universidade Federal de São Paulo, 12231-280, São José dos Campos, São Paulo, Brazil

ABSTRACT: Atomistic molecular dynamics simulations were employed to investigate the solvation properties of the fullerene C_{60} in binary water/dimethyl sulfoxide (DMSO) mixtures. Structural analysis indicates a preferential solvation with the predominance of DMSO molecules in the first solvation shell for the solutions with low concentrations of DMSO. PMF calculations indicate a maximization of the hydrophobic interaction at low concentrations of DMSO. The contact minima indicate a tendency of aggregation of these nanostructures in water/DMSO mixtures and in the both pure solvents. The free energy of solvation suggests that the hydrophobicity of the fullerene increases monotonically with the increase of DMSO concentration. This result is incompatible with the polarity of DMSO, since it was expected that increasing the concentration of DMSO entailed an increase of C_{60} solubility.

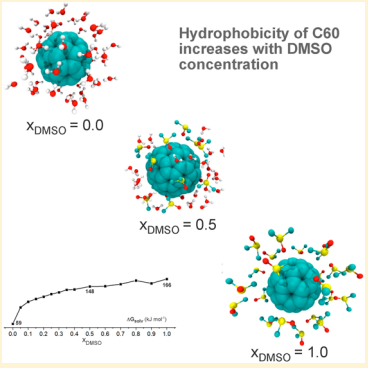

INTRODUCTION

Aqueous mixtures of organic solvents arouse particular interest in biochemistry because of the possibilities of application in various areas.[1−10] One of the binary mixtures that present the most remarkable properties is the aqueous solution of dimethylsulfoxide (DMSO). Such solutions have biological properties that allow their use in areas such as cryopreservation of biological material,[11−13] in addition to acting on change in enzyme activity and protein stability, both in different concentration ranges of cosolvent.[14,15]Additionally, similar to ionic liquids, these mixtures also offer a different reaction medium. These properties are inherently dependent on concentration of DMSO.[1,14,16]

DMSO and water at ambient conditions are miscible in any proportion. As in pure water, where intermolecular interactions are mediated by hydrogen bonds, a complex hydrogen-bonding network from water−water, water−DMSO, and DMSO−DMSO interactions are observed in water/DMSO mixtures.[14,17,18] As this interaction network evolves with composition, binary water/DMSO mixtures have been treated as an environment with adjustable properties. Experiments of X-ray diffraction rejected the idea of a high degree of hydrophobic association in these mixtures.[19,20] DMSO has a large dipole moment along the S−OD bond, which is approximately twice that of water. Other equivalent molecules that have similar mixed sites usually have smaller dipole moments. Soper et al. confirmed the evidence that water molecules form a disordered hydrogen-bonded cage around small apolar groups.[19,20] The hydrogen bond network deforms to avoid regions occupied by small hydrophobic species. Mancera et al., using molecular simulations, investigated the hydrophobic and hydrophilic behavior of the water/DMSO mixtures.[17,21] Their simulations indicate the existence of an enhancement in the structure of water around both the hydrophilic and hydrophobic portions of DMSO with respect to the bulk of the solution. Furthermore, they found that the balance between the hydrophilic and hydrophobic interactions clearly favors the former. Recent works have reported the solvation of small molecules at various DMSO concentrations.[14,15,22,23] Bangchi showed that several physical properties of the mixture, particularly hydrophobicity, exhibit deviations at low DMSO concentrations.[14] For example, methane molecule exhibits a more pronounced hydrophobicity at a molar fraction, $x_{DMSO} \sim 0.15$. The hydrophobicity was defined in terms of hydrophobic pair interaction between the solute particles calculated from the potential of mean force (PMF). This methodology provides a detailed description of the hydrophobic interaction and also provides information about the hydrophobic effect.

It was observed for small organic molecules, such as methane, that the solvation in binary mixtures is favored in water-poor solutions.[14,15,22−24] In the case of the solvation of hydrophobic nanostructures, such as C_{60} fullerene, in water/DMSO binary mixtures there are neither computational nor experimental reports available. However, as the C_{60} fullerene is a more hydrophobic solute than methane, we expect a different behavior of the solvophobic interaction in such mixtures. In this work, molecular dynamics simulations are used to investigate the thermodynamic behavior of solvation C_{60} in aqueous solutions of DMSO varying the molar fraction of cosolvent,

Received: November 27, 2013
Revised: February 10, 2014
Published: March 5, 2014

x_{DMSO}, from 0 to 1. The tendency of C_{60} aggregation in these mixtures was also investigated using potential mean force and free energy calculations at each concentration studied. We underline that solvent polarity considerations are unable to describe the observed solvation pattern.

COMPUTATIONAL DETAILS

Cubic computational cells containing a C_{60} molecule immersed in mixtures of water and DMSO with molar fraction of DMSO varying between x_{DMSO} = 0 (pure water) and x_{DMSO} = 1 (pure DMSO) for each solution. A representative configuration of the first solvation shell is shown in Figure 1.

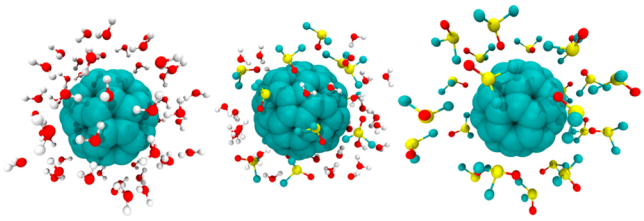

Figure 1. C_{60} fullerene and its first solvation shell. (Left) C_{60} in pure water x_{DMSO} = 0, (center) C_{60} in the water/DMSO mixture (x_{DMSO} = 0.5), and (right) C_{60} in pure DMSO (x_{DMSO} = 1).

The simulations were performed in the isothermal−isobaric ensemble (NPT) under ambient conditions (T = 298 K and P = 1 atm). The water molecule was represented using the three-site TIP3P[25] nonpolarizable model. The dimethyl sulfoxide molecule was represented using four-site model, where each methyl group was considered as a single interaction site.[26] The interaction model used to describe the C_{60} molecule was parametrized and validated in previous studies.[27,28] We note that the interactions between C_{60} and water molecules are described exclusively through the LJ interactions between the C_{60} carbon and water oxygen (since our model for C_{60} has no charge and water H atoms does not have LJ σ and ε terms, then there is not solute−solvent LJ interaction). Nevertheless, these models here been satisfactorily used in the description of hydration of the C_{60}. For example, Monticelli employed nonpolarizable additive models to determine thermodynamical properties of C_{60} in pure SPC water.[29] Scheraga calculated the C_{60} dimerization PMF also using additive models and TIP3P water.[30] Other previous studies have calculated hydrating properties of fullerenes using this approach, in both SPC and TIP3P water.[31−33]

The interaction parameters used in this work are summarized in Table 1. The parameters for each molecule were obtained using a physically equivalent procedure to map potential energy surfaces around these particles. Therefore, the models can be safely combined in a single molecular dynamics simulation. We anticipate additive Coulombic interactions among C_{60}, water, and DMSO. The partial Coulombic charges derived from electrostatic potential at the surface of each molecule in vacuum are transferrable to the condensed phase systems. In the course of sampling, all the charges were kept fixed (nonpolarizable approach).

Table 1. Set of Parameters Employed in This Work for the Water, DMSO and C_{60} Molecules

model	atoms	q	σ (nm)	ε(kJ mol^{-1})
TIP3P	O	−0.834	0.3151	0.6364
	H	0.417	0.00	0.00
OPLS	S	0.139	0.356	1.65268
	O	−0.459	0.293	1.17152
	CH_3	0.160	0.381	0.669440
C_{60}	C	0.00	0.3500	0.317984

The solutions were pre-equilibrated during 1 ns and afterward a set of equilibrium properties was determined from production runs of 10 ns. The integration time-step of 2 fs was used, whereas the trajectories were collected every 0.1 ps. The systems were subjected to coupling of temperature and pressure using the velocity rescaling[34] and Parrinello−Rahman[35] schemes with the coupling constants of 0.1 and 1.0 ps, respectively. All bonds were kept fixed by the LINCS algorithm.[36] A cutoff distance of 1.2 nm was employed for Lennard-Jones interactions, whereas the Coulomb interactions were treated using the Particle Ewald Mesh approach.[37]

To calculate the solvation free energy, a thermodynamic integration was employed. For that, a gradual decoupling of the solute molecule from its equilibrium environment was performed 26 simulations were performed corresponding to the increment of coupling parameter, $\Delta\lambda$ = 0.04, whereas λ evolves from 0 to 1. Within each simulation window, the system was equilibrated during 1 ns and then subjected to a production phase of 5 ns to obtain the average of $\langle \partial H(\lambda)/\partial\lambda \rangle_{\lambda}$. The last value is directly related to solvation free energy.

Quantitative information about the association process of fullerene in water/DMSO mixtures can be obtained by calculation of potential of mean force (PMF). PMF is the function that describes how the free energy between two fullerenes varies as we increase the distance between their centers. To calculate the PMF, we employed umbrella sampling technique[38] with weighted histogram analysis method (WHAM).[39] This technique requires a number of restraints to be applied at specific positions along the reaction coordinate (in this case the distance between two fullerene molecules), so that all regions are appropriately sampled. Each simulation with a restrained reference position is referred to as a window simulation. In this work, for each fullerene pair we conducted a series of 20 simulation windows with harmonic restraint of 3000 kJ mol^{-1} nm^{-2} where the separation between the centers of mass was increased from 0.35 to 1.30 nm with 0.05 nm increments. Each simulation was 10 ns long, providing a total simulation time of 200 ns.

All stochastic and molecular dynamics simulations were performed using the GROMACS 4.5 program.[40,41]

RESULTS AND DISCUSSIONS

The nanoscale structure of the fullerene solutions of in water/DMSO mixtures was analyzed by calculating radial distribution function of the center of mass (RDF) for each molar fraction studied. Figure 2a show that the distribution of C_{60}-DMSO (red curve) has higher peak, indicating a high concentration of DMSO molecules near the fullerene surface and that C_{60} is preferentially solvated by DMSO molecules. This feature is confirmed by the comparison of the number of water molecules in the first solvation shell of C_{60} in pure water and in water/DMSO mixtures for all molar fractions investigates (Figure 2b). At this concentration, the number of water molecules in the first solvation shell of C_{60} decreases 2-fold. Another important feature of these solutions is the number of DMSO molecules in

dx.doi.org/10.1021/jp4116639 | J. Phys. Chem. B 2014, 118, 3378−3384

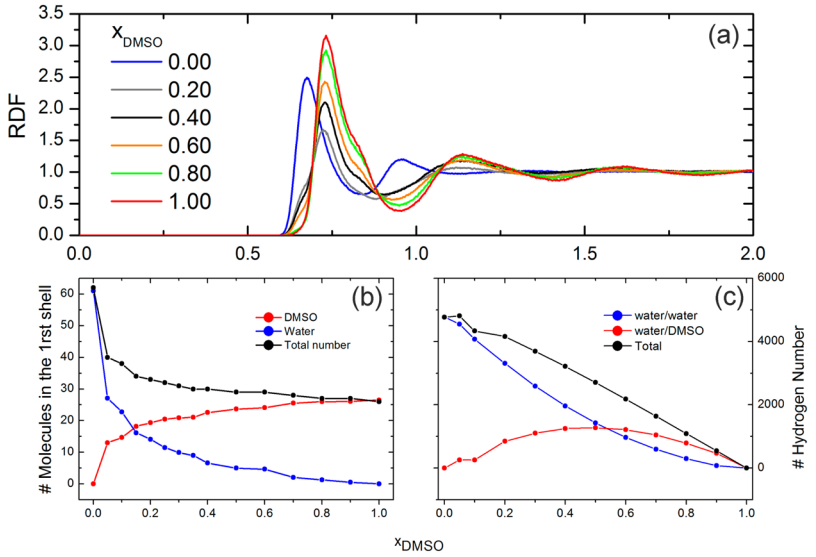

Figure 2. (a) Center-of-mass radial distribution function (RDF) for C_{60} and molecules of the mixtures at selected molar fraction. (b) Partial and total number of molecules in the solvation shell. (c) Average number of H-bonds for water/water and water/DMSO contacts calculated for the bulk mixtures. The structural definition of an H-bond was taken from ref 42.

the first solvation shell, which significantly increases within the range from x_{DMSO} = 0.05 to 0.10, while the opposite is observed for water molecules. The expected aggregation of the DMSO molecules with the increase of x_{DMSO} has a great impact on the energetics of the system. This is closely connected to the hydrogen bonds in the mixtures. Figure 2c shows the average number of hydrogen bonds formed in the mixtures as a function of concentration. It is possible to note a nonuniformity in the region of x_{DMSO} = 0.05−0.10 for the total number of hydrogen bonds. As will be shown further ahead, a maximum for the aggregation tendency of the fullerene C_{60} occurs in this region.

Even for other molar fractions of DMSO, the first peak of the RDF is more significant in relation to the distribution of water molecules. However, this peak height gradually decreases as the concentration of DMSO increases. Furthermore, the position of the first minimum in the C_{60}−water RDF coincides roughly with the first peak of the C_{60}-DMSO RDF, indicating a layered structure of both water and DMSO around the solute. This configuration favors specific intermolecular interactions between the solvent molecules in the vicinity of C_{60}.

The experimental data on transport properties of C_{60} are unavailable. In fact, experimental measurements of the diffusivity of C_{60}, even in pure liquids are scarce. We calculated the diffusion coefficient of the C_{60} fullerene at each studied concentration using the Green−Kubo formula. The diffusion coefficient (D) can be expressed via linear velocity of each interaction site versus time using non-normalized autocorrelation function. Trajectory of 10 ns for each system was recorded, and velocities were saved every 6 fs. Each trajectory was divided into 10 parts, and for each part the diffusion coefficient was obtained using a velocity autocorrelation function of 60 ps. D was obtained as an average over 10 partial calculated values. In Figure 3 we observed a larger diffusion coefficient for C_{60} in water (1.11×10^{-9} m^2s^{-1}) and lesser in DMSO (0.50×10^{-9} m^2s^{-1}). The diffusion of C_{60} in water agrees with the previously simulated values.[43] As the solvent models tend to overestimate the value of D is expected that the diffusion coefficient of C_{60} is also relatively overestimated. Overall, even at low concentrations, the presence of DMSO significantly reduces the diffusion coefficient keeping it on the same plateau ($\sim 0.40 \times 10^{-9}$ m^2s^{-1}) beyond x_{DMSO} = 0.10.

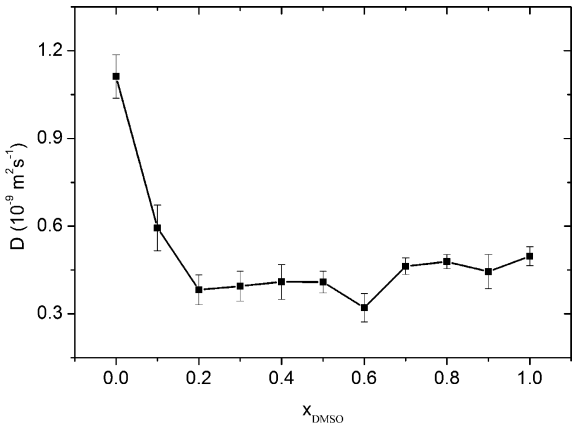

Figure 3. Diffusion coefficient of fullerene C_{60} versus molar fraction of DMSO.

The aggregation of fullerenes and other carbon structures in liquid water have been examined carefully in previous studies.[44,45] In order to understand the trend of aggregation of the fullerene C_{60} in binary mixtures, we calculated PMF for a dimer of C_{60} using the distance between the molecular center-of-masses as reaction coordinate at each DMSO molar fraction.

The depth of contact minimum provides a measure of the solvophobic interaction in solution, containing a hydrophobe,[15] while the difference between the first and second minima dictate whether the direct contact configurations of fullerene C_{60} are more predominant than solvent-separated configurations at different DMSO concentrations. Figure 4 depicts the first minimum, which is located at 0.99 nm. The position of this minimum does not vary as molar fraction of DMSO increases. Both position and the strength of interaction of the C_{60} dimer in pure water are in good agreement with the previous values obtained by Scheraga.[45] In Figure 4 we can see still a second minimum around 1.36−1.39 nm. This minimum,

dx.doi.org/10.1021/jp4116639 | J. Phys. Chem. B 2014, 118, 3378−3384

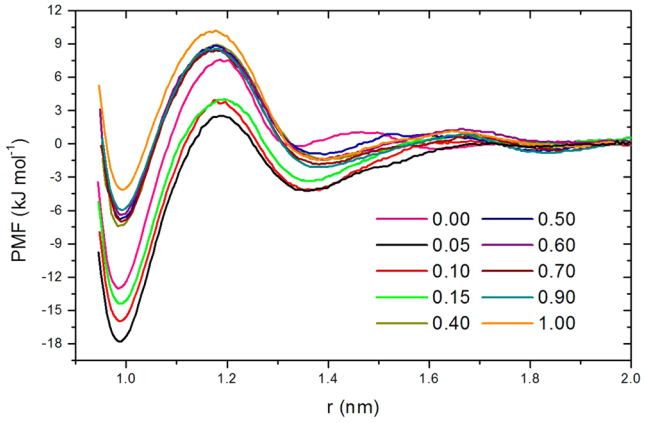

Figure 4. Potential of mean force for a dimer of C_{60} in water/DMSO mixtures for each selected concentration. The curves were adjusted to approach zero at 2.0 nm.

commonly called the solvent separated minimum, corresponds to the distances at which water molecules can enter the space between the two fullerenes.

Figure 5 show a nonideal behavior of binary mixture including a significant increase of hydrophobicity at x_{DMSO} = 0.05. Despite the position of the first and second minima does not vary, its depth experiences major changes. The depth of first minimum reaches its minimum value at 0.05, but significantly increases at higher concentrations. For second minimum, we note a similar behavior, with greater depth related to lower DMSO molar fractions. From the Figure 5 we can observe that the difference between the first and second minima systematically decreases with increasing concentration, without the appearance of a maximum in the hydrophobic tendency for direct contact configurations of fullerene C_{60}, indicating that configurations are separated by more favorable solvent in water-rich solutions. However, this difference reaches its maximum value at x_{DMSO} = 0.05, which suggests the fact that this concentration there is a greater tendency for aggregation of the molecules of C_{60} molecules at this concentration.

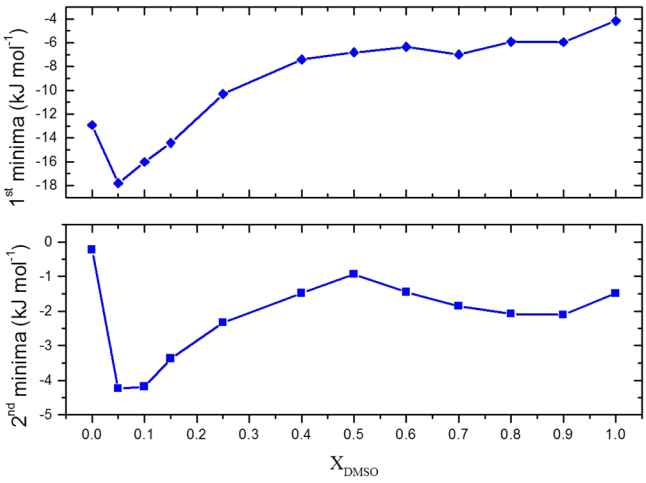

Figure 5. Contact and solvent separated minima for C_{60}−C_{60} dimer in water/DMSO mixtures. The corresponding minimum at various concentrations was obtained from the graphs shown in Figure 4.

It is clear that the behavior of C_{60} in water/DMSO environment reveals unusual characteristics at low concentrations. However, it is different from the findings of Bagchi et al. for methane molecule at these same conditions.[15] A stronger interaction for a dimer of methane molecules was also found at low concentrations. The molar fraction of DMSO was though somewhat higher x_{DMSO} = 0.15, as compared with C_{60}. This principal difference of PMF for C_{60} dimers may be related to its size and spherical shape, which produces a cavity within the solvent with much larger volume compared to the volume in case of methane. In low DMSO concentration solutions, local tetrahedral structure of water is well preserved in the presence of DMSO molecules.[14,18] DMSO molecules tend to associate with each other by methyl−methyl interaction. As methane is a very small hydrophobe, comparable to the DMSO methyl groups, it can behave like a methyl group and facilitate the aggregation of DMSO molecules.[15] Consequently, the anomalies of water−DMSO binary mixture at low concentrations will be well described because there is no so much impact on the DMSO network.[15] In the case of the solvation of C_{60}, this trend is not observed. The presence of the C_{60} (much higher than methane) dramatically affects the DMSO aggregation; additionally, the interaction C_{60}−methyl$_{(DMSO)}$ induces a orientational order in the DMSO molecules at the vicinity of the carbon cage. This orientation will interfere with the hydrogen bonds formed between water molecules network, and the effect of this interference is variable, depending on the concentration of DMSO.

At room temperature, the hydration of small hydrophobic nonpolar particles is dominated by the entropic term, while for larger nonpolar particles, hydrophobicity is dominated by enthalpic factors.[46] The crossing from small to large molecular scale, in terms of hydrophobic interactions, was predicted to occur at the nanometer scale.[46] The size of the fullerene puts it exactly at the meeting point between these two length scales. Studies show, however, that fullerenes are too large to be treated as conventional hydrophobic molecules, but not large enough to be considered as hydrophobic macroscopic surfaces.[30,46] Here we encounter another peculiarity of solvation of fullerene due to its large size compared the small hydrophobic solutes, such as methane. Figure 6 shows a comparison between the solvation thermodynamics of the two

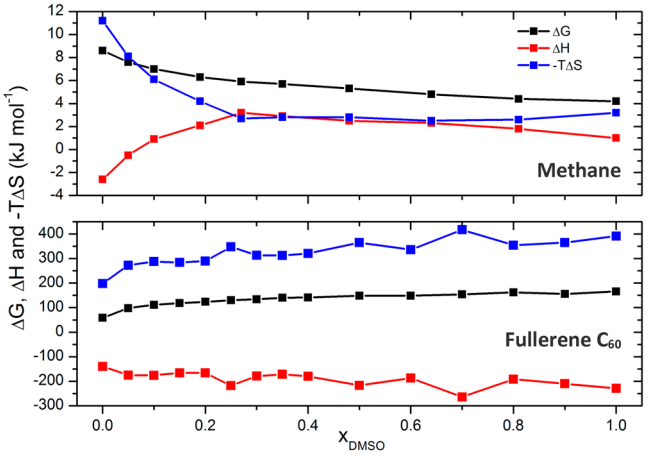

Figure 6. Comparison between the thermodynamics of solvation in mixtures of water/DMSO for two length scales: methane and C_{60}. Entropy, enthalpy and free energy of solvation are presented as a function of molar fraction, x_{DMSO}. Data for methane were adapted from Table 2 of reference 22.

dx.doi.org/10.1021/jp4116639 | J. Phys. Chem. B 2014, 118, 3378−3384

size scales: methane and C_{60}. From Figure 6 we can see that the energetics of both molecules in binary mixtures, differ not only in the order of magnitude (values for the solvation energies of the C_{60}, found here, are about 10 times higher than methane[22]) but also in the nature of their entropic/enthalpy behavior. For methane, the solvation free energy decreases monotonically with concentration, whereas for C_{60} this energy increases. The free energy of solvation for methane in low concentrations DMSO/water mixtures (<0.20) is strongly governed by entropy, while for larger x_{DMSO} values there is an entropic/enthalpic balance (Figure 1). However, for C_{60}, the entropic/enthalpic balance is verified over the whole concentration range, with a slight advantage to the entropic contribution.

The higher values for enthalpy of solvation were found in DMSO-rich solutions. Indeed, one can hypothesize a strong dispersion interaction between sulfur and carbon atoms. This interaction promotes a favorable enthalpy of solvation in the concentrated DMSO solutions. On the other hand, the intense interactions between oxygen atom of water and sulfur atom of DMSO are responsible for a drastic change of entropy. In $x_{DMSO} = 1.0$ system, both oxygen and sulfur belong to dimethyl sulfoxide causing strong antiparallel dipole−dipole association of the solvent molecules. In the $0 < x_{DMSO} < 1$ systems, the discussed interaction additionally include oxygen atoms of water molecules. An alternative explanation involves perturbation of hydrogen bonding network, which is more ramified in water-rich systems, while the energies of water−water and water−DMSO hydrogen bonding are nearly identical, with $r_{O-H} = 0.171$ nm in both solvents. The perturbation of hydrogen bonds brings a significant entropic penalty. Noteworthy, entropic contribution exceeds enthalpic contribution by up to 80%. As a combination of enthalpic and entropic contributions, the free energy of solvation exhibits an unexpected trend for the solvation of C60 in DMSO-rich solutions. The solvation process is driven by entropy, whereas enthalpy contribution is quite modest (Figure 6).

It was expected that the addition of DMSO molecules favor solvation of C_{60}, as observed by Özal, upon solvation of methane in the same mixtures.[22] However, out study unveils that solvation free energy increases monotonously as x_{DMSO} increases, ranging from 59 kJ mol^{-1} (pure water) to 167 kJ mol^{-1} (pure DMSO). The difference, $\Delta\Delta G_{wat\text{-}DMSO} \sim 100$ $kJmol^{-1}$, indicates hydrophobicity increase of C_{60} in DMSO-rich solutions. This finding suggests that solvent polarity is not sufficient to characterize C_{60} solvation. Counterintuitively, solvation of C_{60} is more favorable in water, despite a higher polarity of water as compared to DMSO. It is necessary to consider other solvent parameters including thermodynamics of its miscibility. DMSO possesses oxygen with an electron lone pair responsible for hydrogen bonding with neighboring molecules, sulfur atoms and oxygen also interact strongly in pure liquid, forming continuous molecular associates. This stable network of intermolecular interactions can be destabilized by the presence of a nanometric hydrophobe, such as C_{60}. It is forced to rearrange in order to recover the solvation structure, thus increasing the total entropy of the system. The most intriguing conclusion is that enthalpy gain, brought by DMSO admixture (Figure 6), is well overcompensated by entropy penalty, coming from the fullerene solvation in the resulting mixture. Since polarity of solvent does not account for entropy of solvation/mixing, it is unable to adequately predict how mixed solvents influence solubility of hydrophobes.

We support the predictions of the empirical force fields by hybrid density functional theory (DFT) calculations. Omega B97D functional was employed,[47] and the system's wave function was approximated using the 6-31G(d) basis set. The dispersion correction, which is of high importance for these systems, is implicitly treated within the selected DFT functional. The geometries of the fullerene containing systems were optimized with the convergence criterion of 10^{-8} Ha. The resulting binding energies were corrected with respect to basis set superposition error (15−20%). In order to compare water and DMSO, we converted the obtained energies into kJ m^{-3} using the information about liquid densities. The solution of fullerene was hereby assumed to be infinitely diluted one. The interactions between the solvent molecules and the fullerene were assumed to be additive. The resulting binding energy for the C_{60}−water system is 328 kJ m^{-3}, while it is 839 kJ m^{-3} for the C_{60}−DMSO system. Indeed, the binding energy of the fullerene with a unit volume of DMSO appears to be 2.5 times higher than with water. Both binding energies are quite small in absolute values being inferior to water−water, DMSO−DMSO, and water−DMSO binding. This result is in good agreement with the selected empirical models and supports a reliability of the above-reported numerical findings. The binding energy can be directly related to the enthalpic factor (Figure 6) obtained in the molecular dynamics simulations. Additionally, this effect can also be seen through the direct interaction between DMSO and water molecules with fullerene. Figure 7 shows a scan for

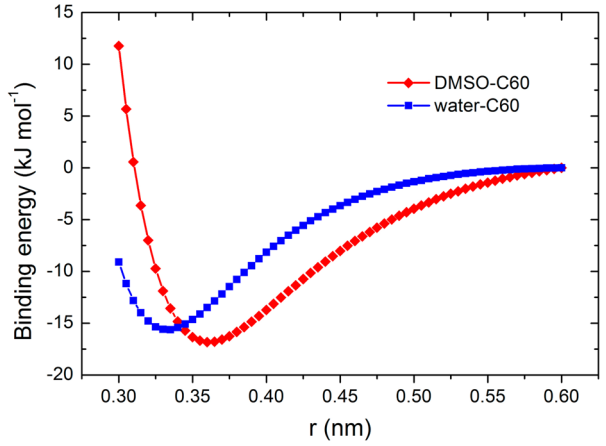

Figure 7. Single-point potential energy as a function of separation distance for the DMSO−C_{60} and water−C_{60} systems. Calculation at the DFT(wB97D)/6-31(d) level of theory.

the binding energy as a function of separation distance for the DMSO−C_{60} and water−C_{60} systems. We observed that the DMSO−C_{60} interaction is about 2 kJ mol^{-1} stronger than water−C_{60} interaction; this is a key factor for the preferential solvation of C_{60} by DMSO.

CONCLUSIONS

In this work solvation properties of the fullerene C_{60} in water/DMSO binary mixtures were investigated, both in structural and energetics terms. The structure revealed a predominance of the DMSO molecules in the C_{60} first solvation shell for solutions with low concentrations of DMSO. The number of DMSO molecules in the first solvation shell increases uniformly, reaching a constant value at high concentrations of DMSO. PMF calculations investigate the association tendency

dx.doi.org/10.1021/jp4116639 | J. Phys. Chem. B 2014, 118, 3378−3384

of C_{60} dimer in these mixtures. The contact minimum of the PMF indicates a tendency of aggregation of these nanostructures in water/DMSO mixtures at any composition. The maximization of hydrophobic interaction was observed at low concentrations of DMSO (x_{DMSO} = 0.05), unlike the previous results for solvation of methane, in which maximization occurred at x_{DMSO} = 0.15. Solvation free energy calculations showed an opposite behavior to that observed for small hydrophobes. We found that the hydrophobicity of the fullerene increases monotonically with DMSO concentration increase. This behavior contradicts the polarity of DMSO, since it possesses significantly lower dielectric constant than water. One can speculate that DMSO forms molecular aggregates throughout the solution, which would lead a large entropic variation to the free energy of solvation, especially in the solutions with high concentrations of DMSO. Since there are no experimental results to characterize the solvation of C_{60} in mixtures, these results follow as a guide to new characterizations of C_{60} in a liquid environment for future endeavors.

AUTHOR INFORMATION

Corresponding Author

*E-mail: fileti@unifesp.br; fileti@gmail.com. Tel: +55 12 3309-9573. Fax: +55 12 3921-8857.

Notes

The authors declare no competing financial interest.

ACKNOWLEDGMENTS

This work was supported by grants from Brazilian agencies FAPESP and CNPq. V.V.C. was supported by the U.S. Department of Energy, Grant No. DE-SC0006527.

REFERENCES

(1) Marcus, Y. *Solvent Mixtures: Properties and Selective Solvation*; CRC Press: Boca Raton, FL, 2002.

(2) Lee, M.-E.; van der Vegt, N. F. A. Does Urea Denature Hydrophobic Interactions. *J. Am. Chem. Soc.* **2006**, *128*, 4948−4949.

(3) van der Vegt, N. F.; Lee, M. E.; Trzesniak, D.; van Gunsteren, W. F. Enthalpy-Entropy Compensation in the Effects of Urea on Hydrophobic Interactions. *J. Phys. Chem. B* **2006**, *110*, 12852−12855.

(4) Ignatova, Z.; Gierasch, L. M. Effects of Osmolytes on Protein Folding and Aggregation in Cells. *Methods Enzymol.* **2007**, *428*, 355−372.

(5) Jain, N. K.; Roy, I. Effect of Trehalose on Protein Structure. *Protein Sci.* **2009**, *18*, 24−36.

(6) Buck, M. Trifluoroethanol and Colleagues: Cosolvents Come of Age. Recent Studies with Peptides and Proteins. *Q. Rev. Biophys.* **1998**, *31*, 297−355.

(7) Murthy, S. S. N. Some Insight into the Physical Basis of the Cryoprotective Action of Dimethyl Sulfoxide and Ethylene Glycol. *Cryobiology* **1998**, *36*, 84−96.

(8) Collins, K. D. Charge Density-Dependent Strength of Hydration and Biological Structure. *Biophys. J.* **1997**, *72*, 65−76.

(9) Timasheff, S. N. Protein-Solvent Preferential Interactions, Protein Hydration, and the Modulation of Biochemical Reactions by Solvent Components. *Proc. Natl. Acad. Sci. U. S. A.* **2002**, *99*, 9721−9726.

(10) Timasheff, S. N. Control of Protein Stability and Reactions by Weakly Interacting Cosolvents: The Simplicity of the Complicated. *Adv. Protein Chem.* **1998**, *51*, 355−432.

(11) Hughes, Z. E.; Mark, A. E.; Mancera, R. L. Molecular Dynamics Simulations of the Interactions of DMSO with DPPC and DOPC Phospholipid Membranes. *J. Phys. Chem. B* **2012**, *116*, 11911−11923.

(12) Hughes, Z. E.; Mancera, R. L. Molecular Dynamics Simulations of Mixed DOPC−β-Sitosterol Bilayers and Their Interactions with DMSO. *Soft Matter* **2013**, *9*, 2920−2935.

(13) Mandumpal, J. B.; Kreck, C. A.; Mancera, R. L. A Molecular Mechanism of Solvent Cryoprotection in Aqueous DMSO Solutions. *Phys. Chem. Chem. Phys.* **2011**, *13*, 3839−3842.

(14) Roy, S.; Banerjee, S.; Biyani, N.; Jana, B.; Bagchi, B. Theoretical and Computational Analysis of Static and Dynamic Anomalies in Water−DMSO Binary Mixture at Low DMSO Concentrations. *J. Phys. Chem. B* **2011**, *115*, 685−692.

(15) Banerjee, S.; Roy, S.; Bagchi, B. Enhanced Pair Hydrophobicity in the Water−Dimethylsulfoxide (DMSO) Binary Mixture at Low DMSO Concentrations. *J. Phys. Chem. B* **2010**, *114*, 12875−12882.

(16) Catalan, J.; Diaz, C.; Garcia-Blanco, F. Characterization of Binary Solvent Mixtures of DMSO with Water and Other Cosolvents. *J. Org. Chem.* **2001**, *66*, 5846−5852.

(17) Mancera, R. L.; Chalaris, M.; Refson, K.; Samios, J. Molecular Dynamics Simulations of Dilute Aqueous DMSO Solutions. A Temperature-Dependence Study of the Hydrophobic and Hydrophilic Behaviour around DMSO. *Phys. Chem. Chem. Phys.* **2004**, *6*, 94−102.

(18) Zhang, N.; Li, W.; Chen, C.; Zuo, J. Molecular Dynamics Simulation of Aggregation in Dimethyl Sulfoxide−Water Binary Mixture. *Comput. Theor. Chem.* **2013**, *1017*, 126−135.

(19) Soper, A. K.; Luzar, A. Orientation of Water Molecules around Small Polar and Nonpolar Groups in Solution: A Neutron Diffraction and Computer Simulation Study. *J. Phys. Chem.* **1996**, *100*, 1357−1367.

(20) Luzar, A.; Soper, A. K.; Chandler, D.; Luzar, A.; Soper, A. K.; Chandler, D. "Combined Neutron Diffraction and Computer Simulation Study of Liquid Dimethyl Sulphoxide", Journal of Chemical Physics, 1993, 99, 6836. *J. Chem. Phys.* **1993**, *99*, 044502.

(21) Mancera, R. L.; Chalaris, M.; Samios, J. The Concentration Effect on the Behaviour of Dilute Aqueous Dmso Solutions. A Computer Simulation Study. *J. Mol. Model.* **2004**, *110*, 147−153.

(22) Ozal, T. A.; van der Vegt, N. F. Confusing Cause and Effect: Energy-Entropy Compensation in the Preferential Solvation of a Nonpolar Solute in Dimethyl Sulfoxide/Water Mixtures. *J. Phys. Chem. B* **2006**, *110*, 12104−12112.

(23) Roy, S.; Bagchi, B. Solvation Dynamics of Tryptophan in Water−Dimethyl Sulfoxide Binary Mixture: In Search of Molecular Origin of Composition Dependent Multiple Anomalies. *J. Chem. Phys.* **2013**, *139*, 034308.

(24) Lee, M. E.; Van der Vegt, N. F. A. Molecular Thermodynamics of Methane Solvation in *tert*-Butanol−Water Mixtures. *J. Chem. Theory Comput.* **2007**, *3*, 194−200.

(25) Jorgensen, W. L.; Chandrasekhar, J.; Madura, J. D.; Impey, R. W.; Klein, M. L. Comparison of Simple Potential Functions for Simulating Liquid Water. *J. Chem. Phys.* **1983**, *79*, 926−935.

(26) Zheng, Y.-J.; Ornstein, R. L. A Molecular Dynamics and Quantum Mechanics Analysis of the Effect of DMSO on Enzyme Structure and Dynamics: Subtilisin. *J. Am. Chem. Soc.* **1996**, *118*, 4175−4180.

(27) Rivelino, R.; Maniero, A. M.; Prudente, F. V.; Costa, L. S. Theoretical Calculations of the Structure and UV−Vis Absorption Spectra of Hydrated C_{60} Fullerene. *Carbon* **2006**, *44*, 2925−2930.

(28) Maciel, C.; Fileti, E. E.; Rivelino, R. Note on the Free Energy of Transfer of Fullerene C_{60} Simulated by Using Classical Potentials. *J. Phys. Chem. B* **2009**, *113*, 7045−7048.

(29) Monticelli, L. On Atomistic and Coarse-Grained Models for C_{60} Fullerene. *J. Chem. Theory Comput.* **2012**, *8*, 1370−1378.

(30) Makowski, M.; Czaplewski, C.; Liwo, A.; Scheraga, H. A. Potential of Mean Force of Association of Large Hydrophobic Particles: Toward the Nanoscale Limit. *J. Phys. Chem. B* **2010**, *114*, 993−1003.

(31) Li, L. W.; Bedrov, D.; Smith, G. D. Water-Induced Interactions between Carbon Nanoparticles. *J. Phys. Chem. B* **2006**, *110*, 10509−10513.

(32) Li, L.; Bedrov, D.; Smith, G. D. A Molecular-Dynamics Simulation Study of Solvent-Induced Repulsion between C_{60} Fullerenes in Water. *J. Chem. Phys.* **2005**, *123*, 204504.

(33) Hotta, T.; Kimura, A.; Sasai, M. Fluctuating Hydration Structure around Nanometer-Size Hydrophobic Solutes. I. Caging and Drying

around C_{60} and $C_{60}H_{60}$ Spheres. *J. Phys. Chem. B* **2005**, *109*, 18600−18608.
(34) Bussi, G.; Donadio, D.; Parrinello, M. Canonical Sampling through Velocity Rescaling. *J. Chem. Phys.* **2007**, *126*, 014101.
(35) Parrinello, M.; Rahman, A. Polymorphic Transitions in Single Crystals: A New Molecular Dynamics Method. *J. Appl. Phys.* **1981**, *52*, 7182−7190.
(36) Hess, B.; Bekker, H.; Berendsen, H. J. C.; Fraaije, J. LINCS: A Linear Constraint Solver for Molecular Simulations. *J. Comput. Chem.* **1997**, *118*, 1463−1472.
(37) Darden, T.; York, D.; Pedersen, L. Particle Mesh Ewald: An *N*·log(*N*) Method for Ewald Sums in Large Systems. *J. Chem. Phys.* **1993**, 10089−10092.
(38) Torrie, G. M.; Valleau, J. P.; Torrie, G. M.; Valleau, J. P. Nonphysical Sampling Distribution in Monte Carlo Free Energy Estimation: Umbrella Sampling. *J. Comput. Phys.* **1977**, *23*, 187−189.
(39) Kumar, S.; Bouzida, D.; Swendsen, R. H.; Kollman, P. A.; Rosenberg, J. M. The Weighted Histogram Analysis Method for Free-Energy Calculations on Biomolecules 0.1. The Method. *J. Comput. Chem.* **1992**, *13*, 1011−1021.
(40) Lindahl, E.; Hess, B.; Van Der Spoel, D. GROMACS 3.0: A Package for Molecular Simulation and Trajectory Analysis. *J. Mol. Model.* **2001**, *7*, 306−317.
(41) Berendsen, H. J. C.; Vanderspoel, D.; Vandrunen, R. GROMACS - a Message-Passing Parallel Molecular-Dynamics Implementation. *Comput. Phys. Commun.* **1995**, *91*, 43−56.
(42) Mancera, R. L.; Buckingham, A. D. Temperature Effects on the Hydrophobic Hydration of Ethane. *J. Phys. Chem.* **1995**, *99*, 14632−14640.
(43) Chopra, G.; Levitt, M. Remarkable Patterns of Surface Water Ordering around Polarized Buckminsterfullerene. *Proc. Natl. Acad. Sci. U. S. A.* **2011**, *108*, 14455−14460.
(44) Maciel, C.; Malaspina, T.; Fileti, E. E. Prediction of the Hydration Properties of Diamondoids from Free Energy and Potential of Mean Force Calculations. *J. Phys. Chem. B* **2012**, *116*, 13467−13471.
(45) Makowski, M.; Czaplewski, C.; Liwo, A.; Scheraga, H. A. Potential of Mean Force of Association of Large Hydrophobic Particles: Toward the Nanoscale Limit. *J. Phys. Chem. B* **2010**, *114*, 993−1003.
(46) Southall, N. T.; Dill, K. A. The Mechanism of Hydrophobic Solvation Depends on Solute Radius. *J. Phys. Chem. B* **2000**, *104*, 1326−1331.
(47) Chai, J. D.; Head-Gordon, M. Long-Range Corrected Hybrid Density Functionals with Damped Atom−Atom Dispersion Corrections. *Phys. Chem. Chem. Phys.* **2008**, *10*, 6615−6620.